

# The dynamics of the tropical cyclone core

H.E. Willoughby, Hurricane Research Division, AOML/NOAA, USA  
(Manuscript received February 1988; revised June 1988)

The core of a tropical cyclone occupies the inner 100-200 km of the vortex. It is dominated by a cyclonic primary circulation in balance with a nearly axisymmetric, warm core low pressure anomaly. Superimposed on the primary circulation are weaker asymmetric motions and an axisymmetric secondary circulation. The asymmetries, which may be either internal gravity waves or Rossby waves, modulate precipitation and cloud into trailing spirals. The axisymmetric secondary circulation, driven by latent heat release and surface friction, comprises the following parts: surface inflow that extracts latent heat from the sea and replaces the frictional loss of angular momentum ( $M$ ) to the sea; diabatically forced deep inflow that supplies an excess of  $M$  above frictional loss; the eyewall, an outward sloping locus of convective ascent; diabatically forced descent inside the eye; and upper tropospheric outflow. The eyewall usually moves inward as a result of differential adiabatic heating across the wind maximum. Eyewall succession occurs in intense cyclones when two concentric eyewalls are present and the outer replaces the inner.

Because of their semibalanced dynamics, the primary and secondary circulations are relatively simple and well understood. These dynamics are not valid in the upper troposphere where the outflow is comparable to the swirling flow, nor do they apply to the asymmetric motions. Since the synoptic-scale environment appears to interact with the vortex core in the upper troposphere by means of the asymmetric motions, future research should emphasise this aspect of the tropical-cyclone dynamics.

## Introduction

'The eye of the storm' is a metaphor for calm within chaos. The core of a tropical cyclone, encompassing the eye and the inner 100-200 km of the cyclone's 1000-1500 km radial extent, is hardly tranquil; but the great rotational inertia of the swirling wind makes it a region of orderly, though intense, motion.

In the core, the local Rossby number is always  $> 1$  and may be  $> 10^2$ ; air swirling around the centre completes an orbit in less than a pendulum day. The core occupies only 1 to 4 per cent of the cyclone's area, but its strong winds threaten human activities and makes the cyclone's dynamics unique. Except at the upper troposphere outflow level, axisymmetric swirling dominates the flow in the core; asymmetric and radial motions are typically less than 10 per cent of the total wind. The vortex and core lie respectively on the meso- $\alpha$  and meso- $\beta$  spatial scales (as defined by Orlanski 1975). Many features in the core, however, have synoptic time-scales, persisting with little change for (pendulum) days (Malkus *et al.* 1961). Because these long lifetimes represent

tens or hundreds of orbital periods, the flow is balanced and dominated by two-dimensional turbulence (Ooyama 1982). Moreover, at winds  $> 35 \text{ m s}^{-1}$ , the local Rossby radius of deformation is reduced from its normal  $\sim 10^3 \text{ km}$  to a value comparable with the eye radius. In very intense tropical cyclones, the eye radius may approach the depth of the troposphere (15 km), making the aspect ratio unity (Shapiro and Willoughby 1982). Thus, the dynamics near the centre of a tropical cyclone are so exotic that conditions in the core differ from the Earth's day-to-day weather as much as the atmosphere of another planet does.

The small spatial scale and long temporal scale, the dominance of the swirling motion, and the presence of a well-defined centre are great conveniences for observation of the core with radar or from aircraft. The size of the core is comparable to the range of search radars. In a single sortie, an aircraft can spend 6-8 h in the core and traverse it 5-10 times. A series of sorties at one altitude can monitor temporal changes or

simultaneous sorties at different altitudes can make nearly synoptic observations in a coordinate system moving with the vortex centre. The foregoing advantages compound for an aircraft equipped with Doppler radar that senses wind as well as precipitation (Jorgensen *et al.* 1983; Marks and Houze 1984). On the other hand, because the core is smaller than the separation between rawinsonde stations, too few ascents exist to define it, even in a composite analysis. Similarly, a dense cloud rooted in the eyewall updraft usually obscures the core from satellite observation. Thus, aircraft and radar are the most appropriate means for quantitative observation of the core.

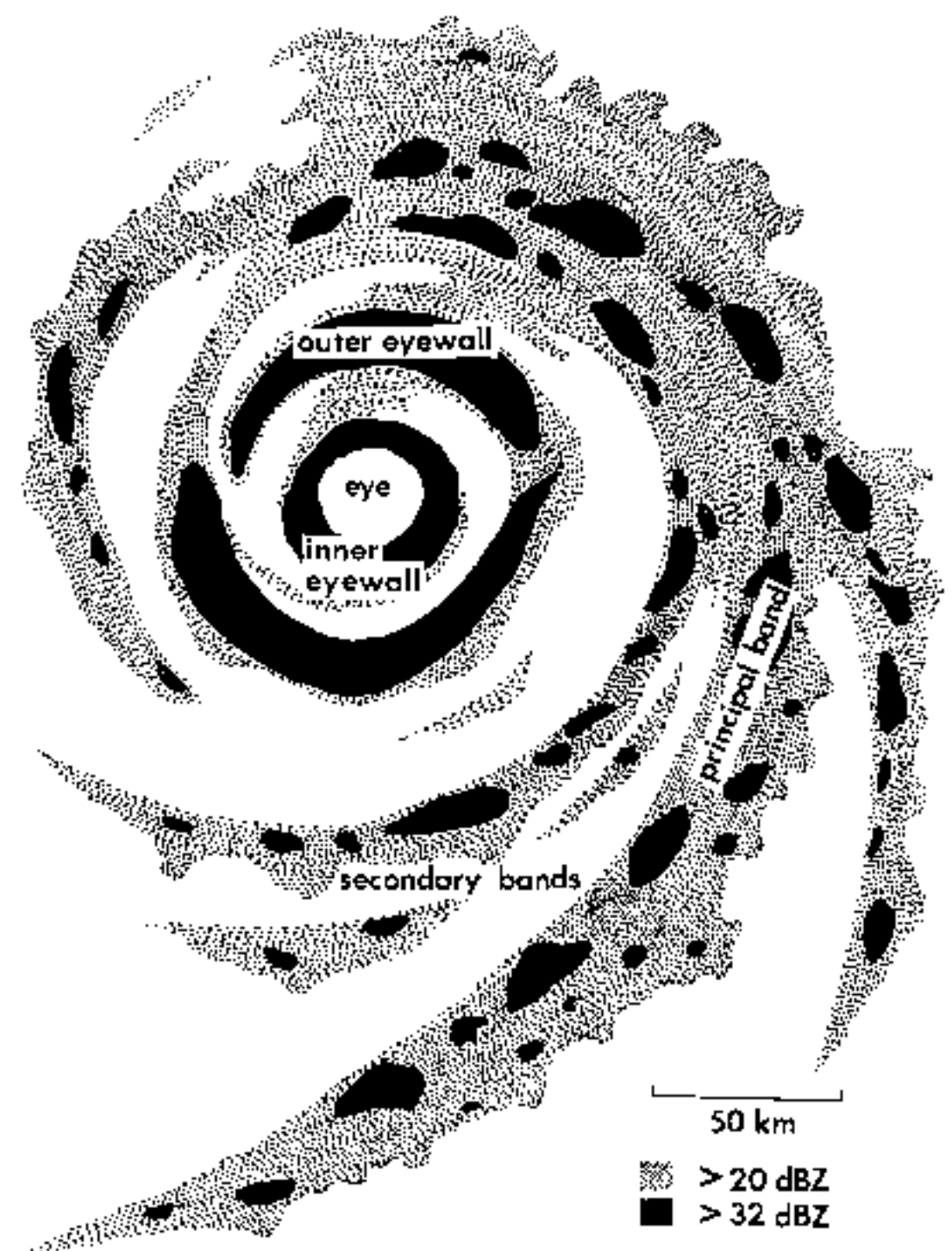
Before the Second World War, tropical cyclone research depended upon surface observations and physical reasoning (*e.g.*, Cline 1926; Deppermann 1947). New observational tools: rawinsondes, radar (Maynard 1945; Wexler 1947), and aircraft (Wood and Wexler 1945; Dunn and Miller 1960) arose near the end of the war. Over the next decade, the outline of the present understanding emerged from analysis of operational observations with the new tools (Riehl 1954). The unusual abundance of Atlantic hurricanes during the 1950s led to special research flights in addition to operational reconnaissance. These flights have continued and have provided a steady flow of observational data (Miller 1967; Anthes 1982). In the late 1980s, comprehension of axisymmetric vortex dynamics and the response to the oceanic heat source has achieved considerable maturity. On the other hand, important unsolved problems remain in the surface boundary layer and the outflow. Although the response to lateral atmosphere forcing has been described through satellite and radiosonde observations (*e.g.* Pfeffer 1958; Miller 1958; Gray 1968; Sadler 1976; Merrill 1985), the dynamics of asymmetrically forced intensity change and motion are poorly understood.

Tropical cyclones' low central pressure results from heating of the tropospheric column by latent heat release (Shaw 1922; Palmen 1948). The process is similar to the 'Thermal Theory of Cyclones,' thought in the 19th century to explain all cyclones, tropical and extratropical (Kutzbach 1979). Moist air flows into the circulation at low levels, ascends in a narrow ring near the centre, where the moisture condenses (Wood and Wexler 1945; Deppermann 1946), and flows outward aloft (Durst and Sutcliffe 1938; Sawyer 1947). The circulation swirling about the vertical axis is the 'primary circulation' of the vortex, and the circulation in the vertical plane is the 'secondary circulation.' The condensationally induced temperature excess often exceeds 10-15°C (Riehl 1948; Hawkins and Rubsam 1968; Hawkins and Imbembo 1976). It extends through the depth of

the troposphere (Haurwitz 1935), and leads to reduced surface pressure. The pressure is typically 1-10 per cent less than that outside the circulation, with a record low of 870 hPa in typhoon *Tip* of 1979 (Dunnavan and Diercks 1980). The rate of condensational heat release, based upon a rainfall rate of 2 mm h<sup>-1</sup> within 100 km of the centre (Marks 1985), is about 5 x 10<sup>13</sup> watts—equivalent to 50 times the worldwide electric generating capacity, or enough heat to warm the atmospheric column at 12°C per day. Most of the realised latent heat sustains the ascending branch of the secondary circulation against adiabatic cooling, but actual temperature changes > 10°C per day must occur in the eyes of rapidly deepening tropical cyclones with observed pressure falls > 2 hPa h<sup>-1</sup> (Holliday and Thompson 1979).

Figure 1 shows a typical pattern of radar returns in the core of a tropical cyclone (Maynard 1945; Wexler 1947). Although radar primarily detects rain, radar images also provide a means for visualisation of the flow. Echo-free areas, such as the eye, generally indicate descent. Convective updrafts generate the reflective condensate, but the echoes also contain precipitation induced downdrafts. The echoes assume two distinct forms: rings that encircle the centre and open

Fig. 1 Schematic illustration of radar reflectivity in a northern-hemisphere tropical cyclone with 50-60 m s<sup>-1</sup> maximum wind.



spirals. The rings and spirals consist of reflectivities  $> 20$  dBZ due to a stratiform rain falling from the overhanging anvil cloud. Within these entities lie smaller echoes of between 32 and 45 dBZ, due to active convection (Parrish *et al.* 1982; Marks 1985). Based upon a typical radar reflectivity-rainfall relationship (Jorgensen and Willis 1982), the stratiform rain rate is about  $0.5 \text{ mm h}^{-1}$  and that in convection is between 3 and  $30 \text{ mm h}^{-1}$ .

Figure 2 shows observed radial profiles of wind and isobaric height in hurricane *Anita* of 1977 at a stage of development corresponding to Fig. 1. The convective rings at the inner and outer eyewall coincide with local maxima of the horizontal wind (Willoughby *et al.* 1982). The lower-tropospheric wind inside the inner eyewall is calm at the centre and increases linearly or faster with radius. The wind outside the outer eyewall decreases inversely as some power of radius, generally thought to be about 0.5, (Hughes 1952; Riehl 1963; Gray and Shea 1973). Idealised functional forms for the radial profile of the swirling wind exist, but do not seem to describe individual cyclones well (Myers 1957; Holland 1980). The convective rings and wind maxima are observed to move slowly inward in response to convective heat release (Willoughby *et al.* 1982). Outside the eye, most of the temperature anomaly is confined to the upper troposphere (Jordan and Jordan 1954; Jordan 1958). Below 500 hPa, the primary circulation has little vertical shear, but in

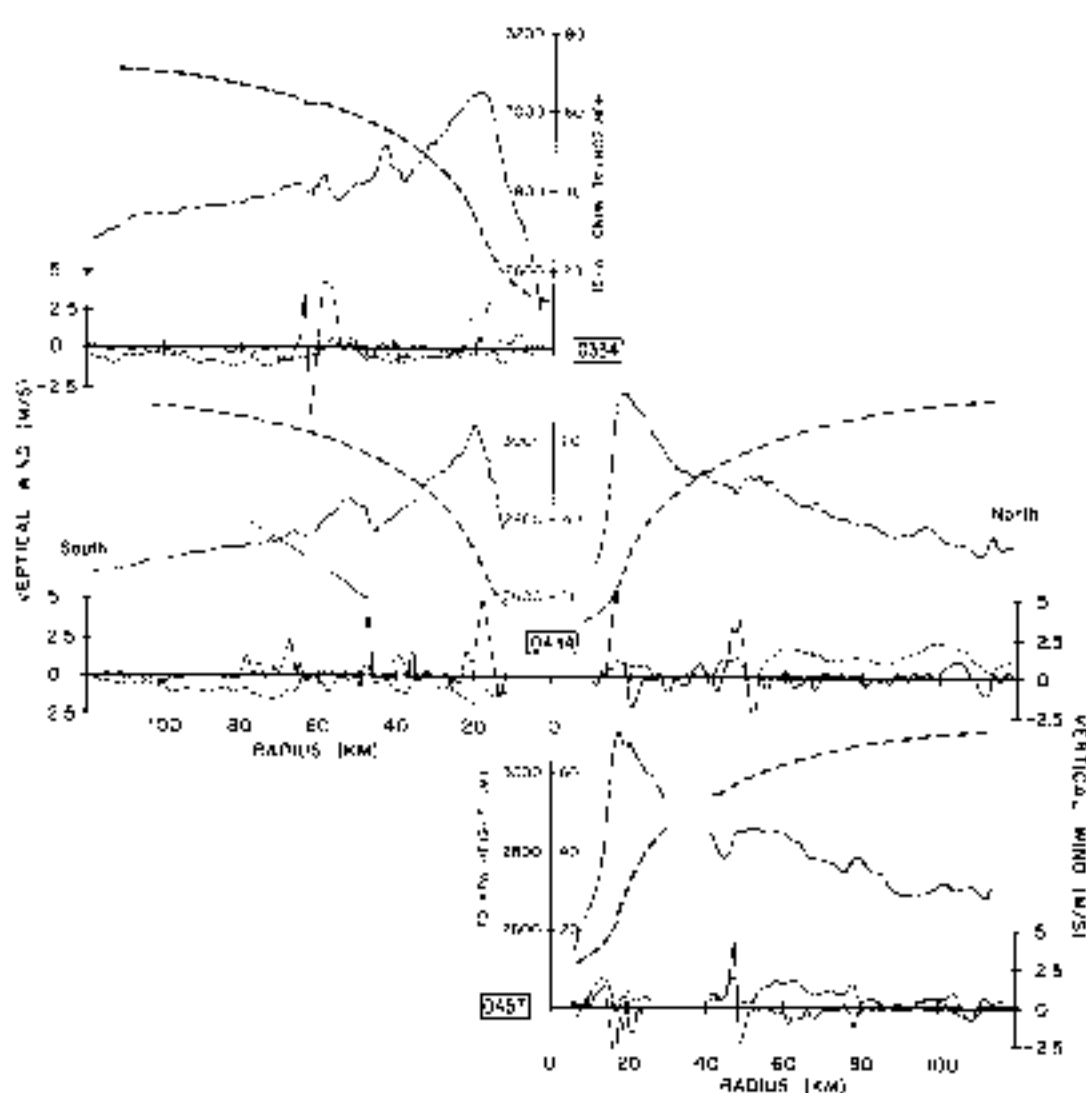
the upper troposphere, it becomes weaker and less symmetric, with the radial outflow a large fraction of the swirling motion. Near the tropopause beyond 200 km radius, the vortex turns anticyclonic (Jordan 1952; Koteswaram 1967) because of angular momentum destruction in the inflow (Riehl 1963).

In Fig. 1, the convective-scale echoes have horizontal dimensions of a few kilometres; the spirals and rings are a few tens of kilometres wide and 100–300 km long; and the axisymmetric circulation occupies the vortex scale. If the mesoscale is defined as having a horizontal scale comparable to the *local* Rossby radius of deformation, the spirals and rings become mesoscale features. The convective motions are neither hydrostatic nor balanced because their horizontal dimensions are less than either the scale height or the local Rossby radius; the mesoscale motions are hydrostatic but not balanced because their horizontal scales are greater than scale height and comparable to the Rossby radius; and the vortex-scale motions are hydrostatic and balanced because their horizontal scales exceed both quantities. As the cyclone intensifies, the Rossby radius and horizontal scale decrease. At extreme intensities, both quantities can become comparable to the depth of the troposphere, obscuring the distinction among convective, mesoscale, and vortex scale motions.

## Asymmetric features

Spiral-shaped patterns of precipitation are the most prominent asymmetric features in Fig. 1. Spiral bands are often considered to be internal gravity waves (*e.g.* Yamamoto 1963), although some bands may be Rossby waves that depend upon the outward decrease in relative vorticity from the cyclone's centre (MacDonald 1968). The earliest radar observations of tropical cyclones revealed spiral bands (Maynard 1945), but many aspects of the bands' formation, internal dynamics, and relation to the symmetric vortex remain unresolved. The bands are typically 5 to 50 km thick and spiral inward toward the centre over a radial interval of 100 to 300 km (Wexler 1947). The precipitation-free lanes between bands are comparable in width with the bands, or somewhat wider. The bands and lanes assume a trailing-spiral shape because the angular velocity of the vortex increases inward and distorts them into equiangular spirals (Abdullah 1976; Senn and Hiser 1959). As the cyclone becomes more intense, the bands turn inward less steeply and come to approximate arcs of circles (Malkus *et al.* 1961; Dvorak 1975). A distinction has to be made between convective bands that spiral around the centre, but do not encircle it, and convective rings that do encircle the centre. Since a band may join

Fig. 2 Observed swirling (chain dashed curve), radial (lighter dashed curve), and vertical wind (solid curve) and 700 hPa (70 kPa) isobaric height (heavier dashed curve) in hurricane *Anita* on 2 September 1977 (Willoughby *et al.* 1982). This situation corresponds roughly to that in Fig. 1.



a ring or appear to wrap around the centre, this distinction is often difficult (Dvorak 1984).

Although some bands appear to move outward (Senn and Hiser 1959), others maintain a fixed location relative to the translating cyclone centre (Malkus *et al.* 1961; Ligda 1955b). Moving bands, or at least the convective 'hot spots' where they join the eyewall, are frequently associated with erratic motion of the cyclone centre (Neuman and Boyd 1962; Jordan 1966; Willoughby and Chelmos 1982; Willoughby *et al.* 1984), and may represent normal modes of the axisymmetric vortex. Stationary bands seem more likely to arise through asymmetric forcing than through hydrodynamic instability. Among possible forcing agents are: asymmetric friction, the gradient of planetary vorticity, horizontal shear of the environmental flow, encounters with topography, and relative motion of the vortex through its environment (Willoughby *et al.* 1982).

Convective elements form near the inner, upwind edges of the bands and move through the bands before dissipating on the outward, downwind edges (Ligda 1955a). Thus, the bands are preferred locations for convection rather than areas of mesoscale condensation. Most bands give rise to widespread stratiform precipitation through horizontal advection of convective debris; indeed some are largely stratiform (Atlas *et al.* 1963; Marks 1985). These scale interactions cast doubt on the conventional view that spiral bands are linear gravity waves.

Another difficulty with the gravity-wave model is the 'frequency problem'. Propagating internal gravity waves exist only in a band of frequencies between the Brunt-Vaisala and local inertia frequencies (Willoughby 1977). Only two classes of trailing-spiral, gravity-wave solutions are possible: waves with tangential wavenumber two or greater that move more slowly than the swirling wind and those with any tangential wavenumber that move faster than the swirling wind. The slowly moving waves propagate wave energy and anticyclonic angular momentum inward, grow at the expense of the mean-flow kinetic energy (Kurihara 1976), and if excited at the periphery of the cyclone, can reach appreciable amplitude. In a sufficiently intense cyclone, these waves can be absorbed at critical radii near the eyewall where their frequency is Doppler shifted to the Brunt-Vaisala frequency (Willoughby 1978). Some observational evidence supports inward propagating waves, and their interaction with the axisymmetric vortex at critical loci seems plausible (Willoughby *et al.* 1984), but they may not be the spiral bands that one sees on radar. Rapidly moving waves appear on radar, but do not draw energy from the mean flow; instead, they probably depend upon release of latent heat. It is also possible that inertial instability (Xu 1983) plays a

role, although observations indicate that only limited instability is present in real tropical cyclones (Black and Anthes 1971).

Motion of the vortex through its surroundings may cause stationary bands (Willoughby *et al.* 1984). In the vortex core, air remains in the circulation for several orbits of the centre; in the outer envelope, the air passes through the circulation in less than the time required for a single orbit. The principal band, a frequently observed stationary spiral, lies along a convergent streamline asymptote (Sherman 1956) that marks the boundary between the core and the envelope. If the environmental flow generally exhibits westerly vertical shear, a cyclone moving with middle-level steering will move eastward through surrounding air at low levels. Thus, the principal band is a 'bow wave' (Beer and Giannini 1980) that marks the limit of the environmental air's penetration on the eastern side. Since its predominant azimuthal wavenumber is one, its governing equation is elliptical or parabolic, making it resemble a convective ring rather than a gravity wave (Willoughby *et al.* 1984). Indeed, observations in hurricanes *Anita* of 1977 (Sheets 1982), and *Alicia* of 1983 (Willoughby 1985) suggest that a convective ring can evolve from the principal band.

## The axisymmetric vortex

The gradual evolution and circularity of the lower-tropospheric vortex indicate, with some observational support (La Seur and Hawkins 1963; Hawkins and Rubsam 1968; Willoughby 1979), that gradient or thermal-wind balance exists in tropical cyclones. At least one argument in favour of large departures from balance (Gray 1962) stemmed from incorrect transformation into moving coordinates. Although the wind may be supergradient where the boundary-layer inflow decelerates under the eyewall, the role of the imbalance in the secondary circulation has been exaggerated.

Eliassen (1951) analysed the secondary circulation induced in a balanced vortex by sources of heat or momentum. By algebraic elimination of the time derivatives from the thermodynamic and tangential momentum equations, he obtained a diagnostic expression for the mass-flow streamfunction in the radius-height plane. Substitution of the diagnosed circulation into the original equations recovered the temporal change. Given gradient balance in tropical cyclones, this analysis provides a context for interpretation of vortex structure and evolution (Smith 1981; Shapiro and Willoughby 1982; Schubert and Hack 1982).

Three parameters determine the character of the secondary circulation; the square of the

Brunt-Vaisala frequency,  $N^2 = (g/\theta)\partial\theta/\partial z$ ; the square of the inertia frequency,  $I^2 = r^{-3}\partial M^2/\partial r$ ; and a measure of baroclinicity,  $B^2 = r^{-3}\partial M^2/\partial z$ , where  $M = vr + fr^2/2$  is the angular momentum,  $v$  the swirling wind,  $\theta$  the potential temperature,  $f$  the coriolis parameter,  $g$  the gravitational acceleration,  $r$  radius, and  $z$  height. Figure 3 shows how changes in  $N^2$ ,  $I^2$ , and  $B^2$  affect the streamfunction. Heating induces an updraft at the source and compensating descent on either side. A cyclonic momentum input induces radial outflow at the source with compensating inflow above and below it. The local Rossby radius is proportional to  $(N/I)$ .  $N^2$  represents the resistance that buoyancy forces offer to vertical motions, and  $I^2$  represents the resistance that inertia forces offer to horizontal motions. When  $N^2 > I^2$  in a barotropic vortex ( $B^2 = 0$ ), the streamfunction forms radially elongated gyres; when  $I^2 > N^2$ , it forms vertically elongated gyres. In a baroclinic vortex, the updraft at a heat source tilts away from the vertical to follow surfaces of constant angular momentum, and the outflow at a momentum source tilts away from the horizontal to follow surfaces of constant potential temperature.

Fig. 3 Streamfunction in the radius height plane induced by: (a) a heat source in a barotropic vortex with  $N^2 > I^2$ , (b) a heat source in a barotropic vortex with  $N^2 < I^2$ , (c) a heat source in a baroclinic vortex, (d) a momentum source in a barotropic vortex with  $N^2 > I^2$ , (e) a momentum source in a barotropic vortex with  $N^2 < I^2$ , (f) a momentum source in a baroclinic vortex (Eliassen 1951).

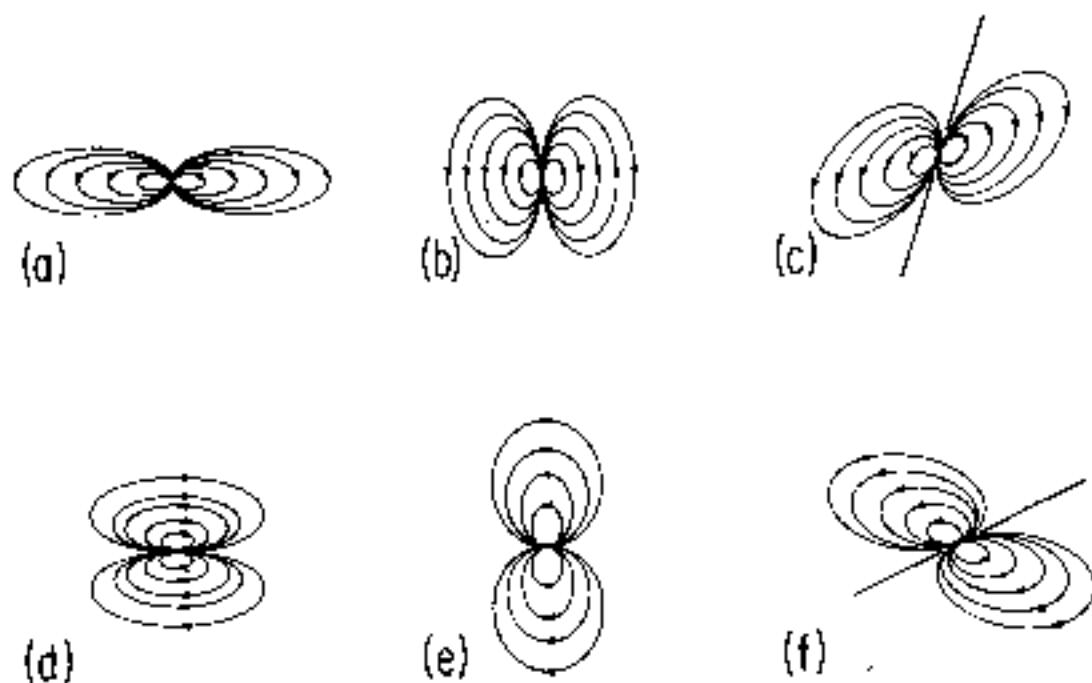
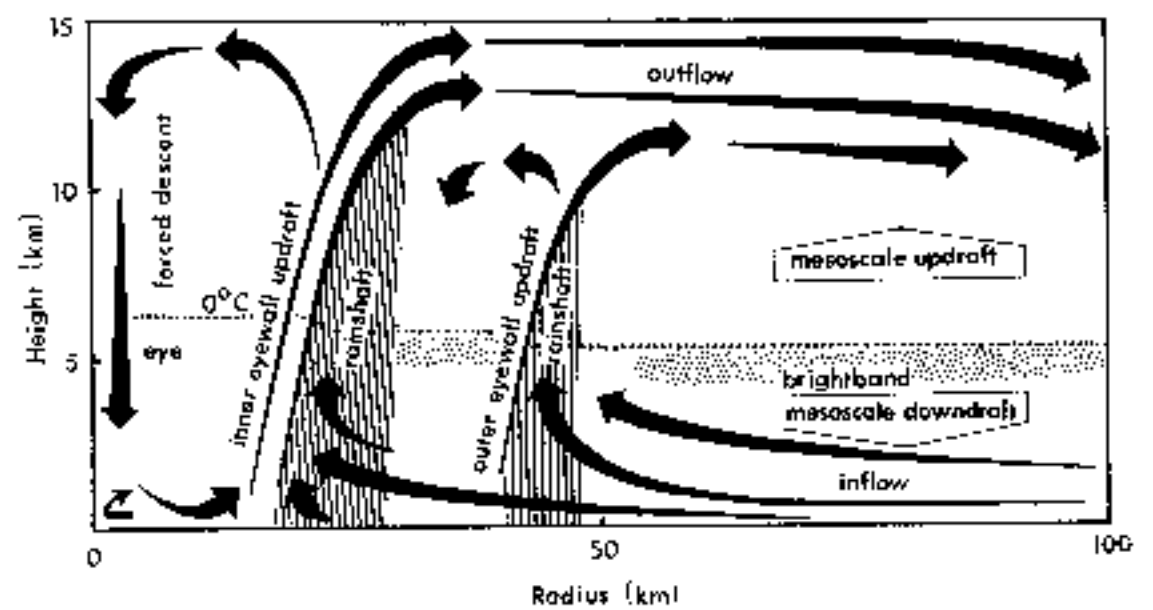


Figure 4 illustrates the observed secondary circulation corresponding to Fig. 1 (Willoughby *et al.* 1982; Jorgensen 1984a, b; Marks and Houze 1987). It arises from the following forcing: an intense frictional angular-momentum sink at the surface, a strong, concentrated condensational heat source at the inner eyewall, a weaker heat source at the outer eyewall, an extended weak heat sink due to precipitation melting along the

Fig. 4 Schematic illustration of the secondary circulation and precipitation distribution for the situation shown in Fig. 1.



brightband, and an extended weak heat source due to condensation in the anvil above the brightband. Since the equation for the secondary circulation is linear, the secondary circulation is a superposition of responses to the individual forcings.

Surface inflow replaces only the angular momentum lost through friction. The inward mass flux depends primarily on the surface stress and is insensitive to the vertical structure of the turbulence (Leslie and Smith 1970). Latent heat transfer to the inflowing air from the warm ocean supplies energy to the updrafts in the eyewalls. In the absence of condensational heating, the air converged in the surface layer would ascend and turn outward at the top of the friction layer instead of rising to the tropopause (Willoughby 1979). It is the combination of frictional surface convergence and heat transfer to the air that sustains the deep secondary circulation. Beyond these simple bulk dynamics, the boundary layer is not well understood.

Figures 1 and 4 show two convective rings: the inner and outer eyewalls. The heat source at each eyewall induces a thermally direct streamfunction gyre outside the eyewall and a thermally indirect gyre inside the eyewall. The direct gyre has inflow in the lower troposphere, ascent at the eyewall, and outflow near the tropopause. The indirect gyre has low-level outflow joining the eyewall updraft, inflow diverging from the eyewall updraft into the eye near the tropopause, and forced descent at the centre of the eye. The direct gyre produces energy and the indirect gyre consumes it. In the direct gyre, where  $v$  decreases with radius,  $I^2$  is much smaller than in the indirect gyre where  $v$  increases with radius. Since  $N^2$  is nearly constant, variation in  $I^2$  controls the shape of the gyres. Outside the eye, the secondary circulation is strong, predominantly horizontal, and extends to large radius; inside the eye, it is weaker, more vertical, and confined horizontally by both large  $I^2$  and the centre boundary. The

foregoing discussion implies that the descent in the eye occurs not through inward momentum diffusion or 'overshooting' of inflowing air (Malkus 1958; Kuo 1959; Gray and Shea 1973) but in response to condensational heating at the eyewall. As Figs 1 and 4 are drawn, the inner eyewall is the stronger. With passage of time in such cases, the outer eyewall usually intensifies, and its indirect cell interferes with the inner eyewall (Willoughby *et al.* 1982) through descent and low-level outflow (Shapiro and Willoughby 1982).

The thermally induced, low-level inflow is distinct from the frictional inflow (Frank 1984). It supplies an excess of angular momentum beyond that required to balance frictional loss at the surface (Ooyama 1982). The eyewall updraft is observed to slope outward along constant angular momentum surfaces (Jorgensen 1984a, b; Marks and Houze 1987). The updraft's slope from the vertical is  $B^2/I^2 = \zeta^{-1}(\partial v/\partial z)$  (Palmen 1956), where  $\zeta$  is the vorticity, and almost invariably exceeds  $45^\circ$ . The observed inclination of the eyewall contradicts claims that the eyewall is vertical (Jordan *et al.* 1960; Shea and Gray 1973).

Outside the eye above the  $0^\circ\text{C}$  isotherm, mesoscale updrafts form through latent heat release; below the  $0^\circ$  isotherm, downdrafts form through melting and precipitation loading. The mesoscale vertical velocities are typically tens of centimetres per second, strong enough to appear in composite analyses of airborne doppler radar observations (Marks and Houze 1987).

The secondary circulation controls the distribution of hydrometeors and radar reflectivity. The ascending motion occurs in numerous individual convective updraft cores. These cover 10 percent of the area in the vortex core and 60 percent of the eyewall. The vertical velocity in the strongest 10 percent of the updraft cores averages  $3\text{--}5\text{ m s}^{-1}$  (Jorgensen *et al.* 1985). Except for 'supercells' observed in tropical storms (Gentry *et al.* 1970; Black 1983), the 'hot towers' with updrafts  $> 20\text{ m s}^{-1}$  once thought to dominate vertical motions in hurricanes (Malkus 1959; Riehl and Malkus 1961; Malkus and Simpson 1964) appear to be rare or absent. Since the updrafts are so weak and incline outward, much of the condensate falls out of them, forming rainshafts outside and below the locus of ascent. About 40 per cent of the rainfall and a larger proportion of the latent heat release occur in the eyewall (Marks 1985). In the rainshaft, precipitation loading, and to a lesser extent evaporation, force convective downdrafts of a few metres per second (Jorgensen *et al.* 1985). The precipitation that remains in the updrafts and reaches the upper troposphere is distributed horizontally by the outflow. It ultimately falls as snow to the melting level where it forms the radar brightband

(Jorgensen 1984a; Marks and Houze 1987). Ice multiplication in the updrafts and entrainment of frozen hydrometeors glaciate nearly all the updrafts by  $-5^\circ\text{C}$  (Black and Hallet 1986).

The asymmetry between the direct and indirect induced gyres causes the convective ring's inward motion. When a condensational heat source lies near the tangential-wind maximum, the total induced subsidence outside the wind maximum will be large, but distributed over a wide area; whereas the total subsidence inside the maximum will be smaller, but concentrated near the heat source. Detailed calculation shows that the adiabatic warming is stronger inside than outside, causing an abrupt change of hydrostatic isobaric height tendency just inside the wind maximum. This radial change in height tendency supports, through the gradient wind relation, the increase in the tangential wind at and just outside the wind maximum, thus making the ring move inward. Kinematically, the speed of inward motion is the ratio of the swirling wind's increase to its radial gradient evaluated on the inward side of the wind maximum. In Fig. 1, both rings are still vigorous, but often when two concentric rings are present, the outer ring subjects the inner ring to subsidence that causes the inner to dissipate. The central pressure may increase if the pressure rise due to the inner ring's destruction exceeds the simultaneous pressure fall due to the outer ring's continuing intensification (Willoughby *et al.* 1982). Notable examples of such eyewall successions are typhoon *Gloria* of 1974 (Holliday 1977) and hurricanes *Allen* of 1980 (Willoughby *et al.* 1982), *Alicia* of 1983, *Diana* of 1984 (Willoughby 1985), and *Gloria* of 1985. Dvorak (1975) describes 'super' ( $v_{\text{max}} > 60\text{ m s}^{-1}$ ) cyclones as often exhibiting circular central dense overcasts surrounded by rings of convective clouds. Thus, *in-situ* and satellite observations support the widespread occurrence of the convective rings. It seems probable that eyewall succession plays a role in many, if not most, intense tropical cyclones. Eyewall succession resembles the sequence of events expected from artificial modification of hurricanes under the STORMFURY hypothesis. This resemblance and the abundance of natural ice raise doubts about STORMFURY's apparently positive results (Willoughby *et al.* 1985).

The definitions of intensity, strength, and size are useful in description of eyewall succession. Intensity is measured by minimum sea-level pressure or maximum wind in the vortex core; strength is the area-averaged swirling wind within 300 km of the centre; and size is the extent of gale force ( $17\text{ m s}^{-1}$ ) wind (Merrill 1984). The observed lack of correlation among changes of intensity, strength, and size (Weatherford 1985) may occur as follows: a tropical cyclone might first experi-

ence increasing intensity when only a single eyewall exists, followed by increasing strength when an outer eyewall forms, then decreasing intensity as the strength continues to increase when the inner eyewall dissipates, and finally increasing intensity again when only the former outer eyewall remains. At the end of the cycle, the tropical cyclone would be larger, more intense, and stronger, but the timing of the changes would be out of phase.

The balanced-vortex model may illuminate some of these changes in tropical cyclones (Holland and Merrill 1984). Convective heating near the centre of the vortex is responsible for intensity changes. Low-altitude momentum sources, that are unable to penetrate to the vortex centre because of the large inertial stability of the lower troposphere, cause changes of strength or size, but not of intensity. On the other hand, momentum sources in the inertially labile upper troposphere may control convective instability, and hence intensification, through forced ascent and adiabatic upper-tropospheric cooling outside the eye (Merrill 1985).

Although the success of the balanced-vortex model of convective rings indicates that, once a ring has formed, its evolution is largely a function of internal dynamics, environmental conditions may play a role in formation. An inward moving, synoptic-scale surge of inflow and ascent may have been the precursor of the initial eyewall of hurricane *Agnes* of 1972 (Molinari and Skubis 1985). Similar developments occur frequently in satellite imagery (Dvorak 1975). Despite these intriguing observations, the question of origin remains unresolved.

## Summary

The accepted paradigm for tropical cyclone dynamics is a warm core primary circulation sustained by latent heat release. Within the core, the axisymmetric secondary circulation conveys latent heat to the eyewall updraft and converges planetary angular momentum to strengthen the swirling wind and replace frictional losses.

Observations since 1980 have led to refinement of the paradigm. The balance between the primary circulation and the mass field is better than previously thought. The 'semi-balanced' equations predict the following observed aspects of the secondary circulation. Deep inflow outside the eye and descent inside the eye are forced diabatically rather than through momentum transports. Eyewall updrafts slope outward along surfaces of constant angular momentum. Eyewalls, or other convective rings, move inward as a result of differential adiabatic heating between their inside and outside. When two

convective rings are present, the outer supplants the inner, and the cyclone often weakens.

Above the boundary layer in a tropical cyclone, the secondary circulation and distributions of radar reflectivity and hydrometeors bear a striking resemblance to a tropical squall line (Houze and Betts 1981), exhibiting an extensive anvil, mesoscale up and downdrafts and brightband. The strongest convective drafts are a few metres per second rather than tens of metres per second. Because of ice multiplication and entrainment, updrafts are largely glaciated at temperatures below  $-5^{\circ}\text{C}$ .

The vortex asymmetries may be either internal gravity waves or Rossby waves. Their role in the synoptic-scale environment's influence on vortex motion and intensity change, perhaps by means of radial wave momentum fluxes, seems to be a productive topic for future research.

## Acknowledgments

I am grateful to R.W. Burpee and L.J. Shapiro for their thoughtful comments. Some of the material is based upon the reports 'Cloud Band Structure' and 'Convective Rings and Intensity Change' prepared for the WMO/CAS International Workshop on Tropical Cyclones, held 24 November to 7 December 1985 in Bangkok, Thailand.

## References

- Abdullah, A.J. 1966. The spiral bands of a hurricane: a possible dynamic explanation. *J. Atmos. Sci.*, 23, 367-75.
- Anthes, R.A. 1982. *Tropical Cyclones: Their Evolution, Structure and Effects*. American Meteorological Society, Boston, 208 pp.
- Atlas, D., Hardy, K.R., Wexler, R. and Boucher, R.J. 1963. The origin of hurricane spiral bands. *Geofis. Int.*, 3, 123-32.
- Beer, T. and Giannini, L. 1980. Tropical cyclone cloudbands. *J. Atmos. Sci.*, 37, 1511-20.
- Black, P.G. 1983. Tropical storm structure as revealed by stereoscopic photographs from skylab. *Adv. Space Res.*, 2, 115-24.
- Black, P.G. and Anthes, R.A. 1971. On the asymmetric structure of the tropical cyclone outflow layer. *J. Atmos. Sci.*, 28, 1348-66.
- Black, R.A. and Hallett, J. 1986. Observations of the distribution of ice in hurricanes. *J. Atmos. Sci.*, 43, 802-22.
- Cline, I.M. 1926. *Tropical Cyclones*, MacMillan, New York, 301 pp.
- Deppermann, C.E. 1946. Is there a ring of violent upward convection in hurricanes and typhoons? *Bull. Am. met. Soc.*, 27, 6-8.
- Deppermann, C.E. 1947. Notes on the origin and structure of Philippine typhoons. *Bull. Am. met. Soc.*, 28, 399-404.
- Dunn, G.E. and Miller, B.I. 1960. *Atlantic Hurricanes*, LSU Press, Baton Rouge, 326 pp.
- Dunnavan, G.M. and Diercks, J.W. 1980. An analysis of Super Typhoon Tip (October 1979). *Mon. Weath. Rev.*, 108, 1915-23.
- Durst, C.S. and Sutcliffe, R.C. 1938. The importance of vertical motion in the development of tropical revolving storms. *Q. Jl R. met. Soc.*, 64, 75-84.
- Dvorak, V.F. 1975. Tropical cyclone intensity analysis and forecasting from satellite imagery. *Mon. Weath. Rev.*, 103, 420-30.

- Dvorak, V.F. 1984. Tropical cyclone intensity analysis using satellite data. NOAA Technical Report NESDIS 11, U.S. Department of Commerce, Washington, D.C., 47 pp.
- Eliassen, A. 1951. Slow thermally or frictionally controlled meridional circulation in a circular vortex. *Astrophys. Norv.*, 5, 19-60.
- Frank, W.M. 1984. A composite analysis of the core of a mature hurricane. *Mon. Weath. Rev.*, 112, 2401-20.
- Gentry, R.C., Fujita, T.T. and Sheets, R.C. 1970. Aircraft, spacecraft, and radar observations of Hurricane Gladys, 1968. *Int appl. Met.*, 9, 837-50.
- Gray, W.M. 1962. On the balance of forces and radial accelerations in hurricanes. *Q. Jl R. met. Soc.*, 88, 430-58.
- Gray, W.M. 1968. Global view of the origin of tropical disturbances and storms. *Mon. Weath. Rev.*, 96, 669-700.
- Gray, W.M. and Shea, D.J. 1973. The hurricane's inner core region. II. Thermal stability and dynamic characteristics. *J. Atmos. Sci.*, 30, 1565-76.
- Haurwitz, B. 1935. The height of tropical cyclones and the eye of the storm. *Mon. Weath. Rev.*, 63, 45-9.
- Hawkins, H.F. and Rubsam, D.T. 1968. Hurricane Hilda, 1964. II. Structure and budgets of the hurricane on October 1 1964. *Mon. Weath. Rev.*, 96, 617-36.
- Hawkins, H.F. and Imbembo, S.M. 1976. The structure of a small intense hurricane—Inez, 1966. *Mon. Weath. Rev.*, 104, 418-42.
- Holland, G.J. 1980. An analytic model of the wind and pressure profiles in hurricanes. *Mon. Weath. Rev.*, 108, 1212-18.
- Holland, G.J. and Merrill, R.T. 1984. On the dynamics of tropical cyclone structural changes. *Q. Jl R. met. Soc.*, 110, 723-45.
- Holliday, C.R. 1977. Double intensification of Typhoon Gloria, 1974. *Mon. Weath. Rev.*, 105, 523-8.
- Holliday, C.R. and Thompson, A.H. 1979. Climatological characteristics of rapidly intensifying typhoons. *Mon. Weath. Rev.*, 107, 1022-34.
- Houze, R.A. and Betts, A.K. 1981. Convection in GATE. *Rev. Geophys. Space Phys.*, 19, 541-76.
- Hughes, L.A. 1952. On the low-level wind structure of tropical storms. *J. Met.*, 9, 422-8.
- Jordan, C.L. 1958. The thermal structure of tropical cyclones. *Geophysica*, 6, 281-97.
- Jordan, C.L. 1966. Surface pressure variations at coastal stations during the period of irregular motion of Hurricane Carla of 1961. *Mon. Weath. Rev.*, 94, 454-8.
- Jordan, C.L. and Jordan, E.S. 1954. On the mean thermal structure of tropical cyclones. *J. Met.*, 11, 440-8.
- Jordan, C.L., Hurt, D.A. and Lowrey, C.A. 1960. On the structure of Hurricane Daisy on 27 August 1958. *J. Met.*, 17, 337-48.
- Jordan, E.S. 1952. An observational study of the upper wind circulation around tropical storms. *J. Met.*, 9, 340-6.
- Jorgensen, D.P. 1984a. Mesoscale and convective-scale characteristics of mature hurricanes. Part I: General observations by research aircraft. *J. Atmos. Sci.*, 41, 1268-85.
- Jorgensen, D.P. 1984b. Mesoscale and convective-scale characteristics of mature hurricanes. Part II: Inner core structure of Hurricane Allen (1980). *J. Atmos. Sci.*, 41, 1287-1311.
- Jorgensen, D.P. and Willis, P.T. 1982. A Z-R relationship for hurricanes. *Int appl. Met.*, 21, 356-66.
- Jorgensen, D.P., Hildebrand, P.H. and Frush, C.L. 1983. Feasibility test of an airborne pulse-doppler meteorological radar. *Int Clim. appl. Met.*, 22, 744-57.
- Jorgensen, D.P., Zipser, E.J. and LeMone, M.A. 1985. Vertical motions in intense hurricanes. *J. Atmos. Sci.*, 42, 839-56.
- Koteswaram, P. 1967. On the structure of hurricanes in the upper troposphere and lower stratosphere. *Mon. Weath. Rev.*, 95, 541-64.
- Kuo, H.L. 1959. Dynamics of convective vortices and eye formation. *The Atmosphere and Sea in Motion*, B. Bolin, ed., Rockefeller Institute Press, 413-24.
- Kurihara, Y. 1976. On the development of spiral rainbands in a tropical cyclone. *J. Atmos. Sci.*, 33, 940-58.
- Kutzbach, G. 1979. *The Thermal Theory of Cyclones*, American Meteorological Soc., Boston, 255 pp.
- La Seur, N.E. and Hawkins, H.F. 1963. An analysis of Hurricane Cleo (1958) based on data from research reconnaissance aircraft. *Mon. Weath. Rev.*, 91, 694-709.
- Leslie, L.M. and Smith, R.K. 1970. The surface boundary layer of a hurricane II. *Tellus*, 22, 288-97.
- Ligda, M.G.H. 1955a. Analysis of motion of small precipitation areas and bands in the hurricane August 23-28, 1949. Tech. Note No. 3, Department of Meteorology, Massachusetts Institute of Technology, 36 pp.
- Ligda, M.G.H. 1955b. Hurricane squall lines. *Bull. Am. met. Soc.*, 36, 340-2.
- MacDonald, N.J. 1968. The evidence for the existence of Rossby-like waves in the hurricane vortex. *Tellus*, 20, 138-50.
- Malkus, J.S. 1958. On the structure and maintenance of the mature hurricane eye. *J. Met.*, 15, 337-49.
- Malkus, J.S. 1959. Recent developments in studies of penetrative convection and an application to hurricane cumulonimbus towers. *Cumulus Dynamics*, C. E. Anderson, ed., Pergamon Press, 65-83.
- Malkus, J.S., Ronne, C. and Chaffee, M. 1961. Cloud patterns in Hurricane Daisy, 1958. *Tellus*, 13, 8-30.
- Malkus, J.S. and Simpson, R.H. 1964. Note on the potentialities of cumulonimbus and hurricane seeding experiments. *Int appl. Met.*, 3, 470-5.
- Marks, F.D. 1985. Evolution of the structure of precipitation in Hurricane Allen (1980). *Mon. Weath. Rev.*, 113, 909-30.
- Marks, F.D. and Houze, R.A. 1984. Airborne Doppler radar observations in Hurricane Debby. *Bull. Am. met. Soc.*, 65, 569-82.
- Marks, F.D. and Houze, R.A. 1987. Inner core structure of Hurricane Alicia from doppler radar observations. *J. Atmos. Sci.*, 44, 1296-1317.
- Maynard, R.H. 1945. Radar and weather. *J. Met.*, 2, 214-26.
- Merrill, R.T. 1984. A comparison of large and small tropical cyclones. *Mon. Weath. Rev.*, 112, 1408-18.
- Merrill, R.T. 1985. Environmental influences on hurricane intensification. Dept. of Atmos. Sci. Paper No. 394, Col. St. Univ., Ft. Collins, 156 pp.
- Miller, B.I. 1958. On the maximum intensity of hurricanes. *J. Met.*, 15, 184-95.
- Miller, B.I. 1967. Characteristics of hurricanes. *Science*, 157, 1389-99.
- Molinari, J. and Skubis, S. 1985. Evolution of the surface wind field in an intensifying tropical cyclone. *J. Atmos. Sci.*, 42, 2865-79.
- Myers, V.A. 1957. Maximum hurricane winds. *Bull. Am. met. Soc.*, 38, 227-8.
- Neuman, S. and Boyd, J.G. 1962. Hurricane movement and variable location of high intensity spot in wall cloud radar echo. *Mon. Weath. Rev.*, 90, 371-4.
- Ooyama, K.V. 1982. Conceptual evolution of the theory and modelling of the tropical cyclone. *J. met. Soc. Japan*, 60, 369-80.
- Orlanski, I. 1975. A rational subdivision of scales for atmospheric processes. *Bull. Am. met. Soc.*, 56, 527-30.
- Palmen, E. 1948. On the formation and structure of tropical hurricanes. *Geophysica*, 3, 26-38.
- Palmen, E. 1956. Formation and development of tropical cyclones. *Proceedings of the Tropical Cyclone Symposium, Brisbane*, Bureau of Meteorology, Melbourne, 213-31.
- Parrish, J.R., Burpee, R.W., Marks, F.D. and Grebe, R.W. 1982. Rainfall patterns observed by digitized radar during the landfall of Hurricane Frederic (1979). *Mon. Weath. Rev.*, 110, 1933-44.
- Pfeffer, R.L. 1958. Concerning the mechanics of hurricanes. *J. Met.*, 15, 113-20.
- Riehl, H. 1948. A radiosonde observation in the eye of a hurricane. *Q. Jl R. met. Soc.*, 74, 194-6.
- Riehl, H. 1954. *Tropical Meteorology*, McGraw-Hill, New York, 392 pp.
- Riehl, H. 1963. Some state relations between wind and thermal structure of steady state hurricanes. *J. Atmos. Sci.*, 20, 276-87.

- Riehl, H. and Malkus, J.S. 1961. Some aspects of Hurricane Daisy, 1958. *Tellus*, 13, 181-213.
- Sadler, J.C. 1976. A role of the tropical upper tropospheric trough in early season typhoon development. *Mon. Weath. Rev.*, 104, 1266-78.
- Sawyer, J.H. 1947. Notes on the theory of tropical cyclones. *Q. Jl R. met. Soc.*, 73, 101-26.
- Schubert, W.H. and Hack, J.J. 1982. Inertial stability and tropical cyclone development. *J. Atmos. Sci.*, 39, 1687-97.
- Senn, H.V. and Hiser, H.W. 1959. On the origin of hurricane spiral rain bands. *J. Met.*, 16, 419-26.
- Shapiro, L.J. and Willoughby, H.E. 1982. The response of balanced hurricanes to local sources of heat and momentum. *J. Atmos. Sci.*, 39, 378-94.
- Shaw, W.N. 1922. The birth and death of cyclones. Reprinted in *Selected Meteorological Papers of Sir Napier Shaw*, Macdonald, London, 1955, pp. 207-21.
- Shea, D.J. and Gray, W.M. 1973. The hurricane's inner core region. I. Symmetric and asymmetric structure. *J. Atmos. Sci.*, 30, 1544-64.
- Sherman, L. 1956. On the wind asymmetry of hurricanes. *J. Met.*, 13, 500-3.
- Sheets, R.C. 1982. On the structure of hurricanes as revealed by research aircraft data. *Intense Atmospheric Vortices*, L. Bengtsson and J. Lighthill eds., Springer-Verlag, New York, 35-49.
- Smith, R.K. 1981. The cyclostrophic adjustment of vortices with application to tropical cyclone modification. *J. Atmos. Sci.*, 38, 2021-30.
- Weatherford, C. 1985. Typhoon Structural Variability. Dept. of Atmos. Sci. Paper No. 391, Col. St. Univ., Ft. Collins, 77 pp.
- Wexler, H. 1947. Structure of hurricanes as determined by radar. *Ann. N.Y. Acad. Sci.*, 48, 821-44.
- Willoughby, H.E. 1977. Inertia-buoyancy waves in hurricanes. *J. Atmos. Sci.*, 34, 1028-39.
- Willoughby, H.E. 1978. A possible mechanism for the formation of hurricane rainbands. *J. Atmos. Sci.*, 35, 838-48.
- Willoughby, H.E. 1979. Forced secondary circulations in hurricanes. *J. geophys. Res.*, 84, 3173-83.
- Willoughby, H.E. 1985. Confirmatory observations of concentric eyes in hurricanes. *Extended Abstracts: 16th Conference on Hurricanes and Tropical Meteorology*, 14-17 May 1985, Houston, Tex., 1-2.
- Willoughby, H.E. and Chelmon, M.B. 1982. Objective determination of hurricane tracks from aircraft observations. *Mon. Weath. Rev.*, 110, 1298-1305.
- Willoughby, H.E., Clos, J.A. and Shoreibah, M.G. 1982. Concentric eye walls, secondary wind maxima, and the evolution of the hurricane vortex. *J. Atmos. Sci.*, 39, 395-411.
- Willoughby, H.E., Marks, F.D. and Feinberg, R.J. 1984. Stationary and moving convective bands in hurricanes. *J. Atmos. Sci.*, 41, 3189-211.
- Willoughby, H.E., Jorgensen, D.P., Black, R.A. and Rosenthal, S.L. 1985. Project STORMFURY: A scientific chronicle 1962-1983. *Bull. Am. met. Soc.*, 66, 505-14.
- Wood, F.B. and Wexler, H. 1945. A flight into the September, 1944 hurricane off Cape Henry, Virginia. *Bull. Am. met. Soc.*, 26, 153-9.
- Xu, Q. 1983. Unstable spiral inertial gravity waves in typhoons. *Sci. Sinica*, 26, 70-80.
- Yamamoto, R. 1963. A dynamical theory of spiral rain band in tropical cyclones. *Tellus*, 15, 155-61.